

ACKNOWLEDGMENTS

We wish to express our appreciation to the ISI,

Calcutta, for use of their computer facilities. One of us (D.C.) is grateful to the CSIR, India, for the award of a Research Fellowship.

¹E. M. Conwell, *High Field Transport in Semiconductors* (Academic, New York, 1967).

²R. Barrie and R. R. Burgess, *Can. J. Phys.* **40**, 1056 (1962).

³H. G. Reik and H. Risken, *Phys. Rev.* **124**, 777 (1961); **126**, 1737 (1962).

⁴N. I. Meyer and M. H. Jorgensen, *J. Phys. Chem. Solids* **26**, 823 (1965).

⁵S. Chou, *J. Phys. Chem. Solids* **31**, 2549 (1970).

⁶D. Chattopadhyay and B. R. Nag, *J. Phys. Chem. Solids* **32**, 2749 (1971).

⁷W. P. Dumke, *Phys. Rev. B* **2**, 987 (1970).

⁸H. B. Levinson, *Fiz. Tverd. Tela* **6**, 2113 (1964)

[*Sov. Phys. Solid State* **6**, 1665 (1965)].

⁹A. Jayaraman and B. B. Kosicki, in *Proceedings of the Ninth International Conference on Physics of Semiconductors* (Nauka, Leningrad, 1968), Vol. 1, p. 47.

¹⁰D. Chattopadhyay and B. R. Nag, *Phys. Status Solidi* **39**, 341 (1970).

¹¹H. Heinrich, K. Lischka, and M. Kriechbaum, *Phys. Rev. B* **2**, 2009 (1970).

¹²W. Fawcett and E. G. S. Paige, *Electron. Letters* **3**, 505 (1967).

¹³E. G. S. Paige, *IBM J. Res. Develop.* **13**, 562 (1969).

¹⁴J. E. Smith, Jr., *Phys. Rev.* **178**, 1364 (1969).

Semiconductor-to-Metal Transition in the Blue Potassium Molybdenum Bronze, $K_{0.30}MoO_3$; Example of a Possible Excitonic Insulator

William Fogle and Jerome H. Perlstein

Department of Chemistry, The Johns Hopkins University, Baltimore, Maryland 21218

(Received 5 February 1971)

The electrical conductivity of the blue-phase potassium molybdenum bronze $K_{0.30}MoO_3$ has been extended down to 4°K. Below 10°K, σ is weakly metallic. Above 10°K, there is an activation energy for conduction of 0.025 eV. Above 180°K, σ becomes metallic again with a discontinuity only in the slope. Several models are suggested to account for the semiconductor-to-metal transition in the absence of an antiferromagnetic Néel point or heat effect at 180°K. Included are the Mott-Hubbard model with a short-range electron-hole attraction proposed by Ramirez, Falicov and Kimball, and the excitonic-insulator model on the semimetallic side. The latter, although semiquantitatively consistent with the electrical conductivity, the Seebeck coefficient, and the weak temperature dependence of the magnetic susceptibility, cannot be distinguished from a correlation-free model involving only a simple lattice distortion on the semimetallic side. The exciton binding energy is calculated to be 0.021 eV in satisfactory agreement with the low-temperature-conductivity activation energy (0.025 eV).

I. INTRODUCTION

The term bronze has been given to a series of highly doped formally mixed-valence metal oxides which in some cases have a very high metallic luster.¹ The tungsten bronzes M_xWO_3 , where M is usually an alkali or alkaline-earth metal, have been the most thoroughly studied. They form simple-cubic perovskite structures each cube corner being occupied by a WO_6 octahedron sharing corners with neighboring octahedra and with the doping atom M sitting in the center of the cube. They are highly metallic with a room-temperature conductivity $\sigma = 2.6 \times 10^4 \Omega^{-1} \text{cm}^{-1}$ for $K_{0.4}WO_3$ as an example. The conductivity is for the most part independent of the kind of dopant and only depends on the dopant's concentration.

The dopant donates its valence electron to the conduction band of the host which in the case of the

tungsten bronzes contains states which are made up of a linear combination of antibonding tungsten $5d(t_{2g})$ orbitals and oxygen $2p_\pi$ orbitals. This bonding scheme for the tungsten bronzes was first suggested by Sienko¹ and further clarified by Goodenough² for the general class of perovskites. Within this general framework it was possible to understand the metallic electrical properties of the tungsten bronzes as arising from an almost-free electron interacting with polar modes of the lattice to form large polarons.³

The significant decrease in the radial extension of the wave function in going from $5d$ to $3d$ raised the question as to the importance of $d(t_{2g})-p_\pi$ overlap for bronzes of the $3d$ -transition-metal oxides. Based on a wealth of information it appears that for the vanadium bronzes $M_xV_2O_5$, the dopant again donates its valence electron to the host, but due to the absence of $d(t_{2g})-p_\pi$ overlap,⁴ the band-

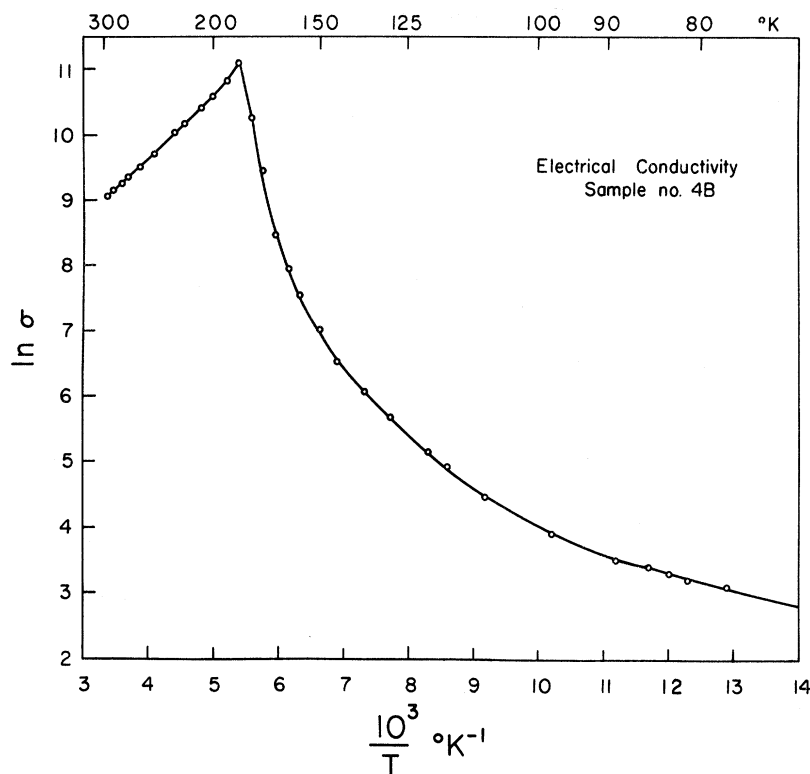


FIG. 1. Natural logarithm of the conductivity vs inverse temperature for $K_{0.30}MoO_3$; 77–300 °K (σ expressed in $\Omega^{-1} \text{cm}^{-1}$).

width is so narrow that electron-phonon interactions dominate producing small polarons which “hop” from one vanadium site to another.⁵

Intermediate between the metallic large-polaron conductivity of the tungsten bronzes and the semiconducting small-polaron behavior of the vanadium bronzes lies the bronzes of the $4d$ transition metals, represented principally by $M_x MoO_3$. Perovskite structures of this bronze with metallic properties exist only for $x > 0.89$ and must be synthesized under high pressure.⁶ The molybdenum bronzes with lower concentration of M can be synthesized by electrolytic techniques as described by Wold, Kunnmann, Arnott, and Ferretti⁷ and were the first molybdenum bronzes to be made as such. With M equal to potassium, the electrolytic technique produces two bronze phases; a blue bronze with the ideal stoichiometry $K_{0.30} MoO_3$ and a red bronze with an ideal stoichiometry $K_{0.33} MoO_3$. The stoichiometries represented here are the theoretical upper limits for the respective monoclinic structures as determined by x-ray crystallography.^{8,9}

Except for its crystal structure, little is known about the properties of the red bronze. It appears to be semiconducting with a room-temperature conductivity $\sigma = 5.1 \times 10^{-5} \Omega^{-1} \text{cm}^{-1}$.⁷

The blue bronze on the other hand has a room-temperature conductivity $\sigma = 7 \times 10^3 \Omega^{-1} \text{cm}^{-1}$ and displays an unusual semiconductor-to-metal tran-

sition at 180 °K as shown in Fig. 1.¹⁰

The crystal structure of this material is side-centered monoclinic, space group $C2/m$, $a = 18.25 \text{ \AA}$, $b = 7.56 \text{ \AA}$, $c = 9.86 \text{ \AA}$, and $\beta = 117^\circ 32'$.⁸ The ideal structural unit consists of ten MoO_6 octahedra

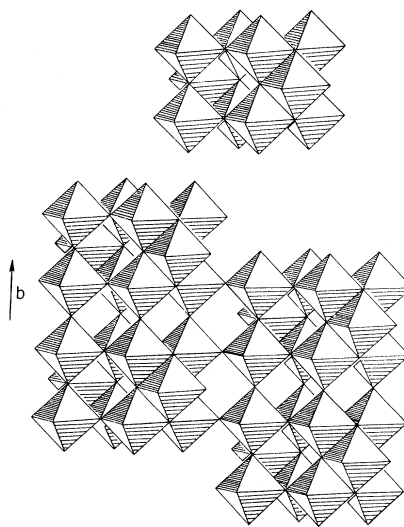


FIG. 2. Top: single cluster of ten edge-sharing MoO_6 octahedra. A molybdenum atom occupies the center of each octahedron with oxygen atoms at the corners. Bottom: repetition of the cluster by corner sharing to form sheets. Arrow indicates direction of b axis.

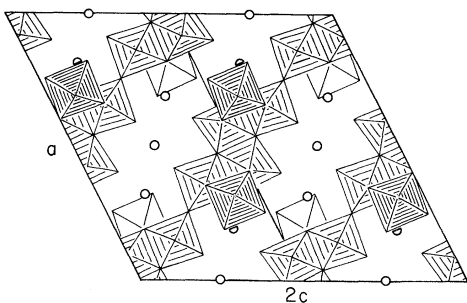


FIG. 3. Projection of $K_{0.30}MoO_3$ structure onto b axis showing distortion of the MoO_6 octahedra in the real structure. Open circles are potassium ions which hold the sheets together.

sharing edges. This cluster of ten octahedra then shares corners only in two directions with other identical clusters forming infinite sheets. The sheets are separated from one another and held together by potassium ions. Figure 2 shows the ideal-sheet formation and Fig. 3 shows the unit cell with the real distorted octahedra projected onto (010). The stoichiometry of the corner-sharing clusters within the sheets is $Mo_{10}O_{30}$. Three potassiums are associated with each cluster giving the ideal stoichiometry $K_{0.30}MoO_3$. In the spirit of the tungsten and vanadium bronzes, it is assumed that the potassium donates its electron to the host structure. Thus, each $Mo_{10}O_{30}$ cluster has three electrons associated with it. Each cluster, on the other hand, is associated with one lattice point in the side-centered-monoclinic cell. Since there are an odd number of electrons per lattice point, one would predict metallic behavior for the blue bronze.

From the shape of Fig. 1 it was not clear to us what the very-low-temperature behavior would be like. If the rapid falloff in slope continued below $77^\circ K$, it would be possible for the ground state to be strongly metallic. This possibility was supported by the magnetic susceptibility from 1.5 to $300^\circ K$ determined by the Gouy method which indicated a Pauli paramagnet at very low temperatures.¹⁰ However, remeasurement of the magnetic susceptibility by the Faraday technique indicates a change from paramagnetic behavior at high temperatures to diamagnetic behavior at low temperatures.¹¹

The present work was therefore initiated to determine the ground state of the blue bronze by measuring the electrical conductivity of single crystals from $4^\circ K$ up.

We have found that the ground state is very weakly metallic. In light of this and in light of the semiconductor-to-metal transition at $180^\circ K$ coupled with a very weakly temperature-dependent magnetic susceptibility, we suggest that the properties of the blue bronze may be due to the formation of an excitonic insulating state on the semimetallic side.

In what follows we will offer some heuristic arguments to show that the electrical conductivity, magnetic susceptibility, and Seebeck coefficient are suggestive of the excitonic-insulator model.

II. EXPERIMENTAL

A. Preparation

Crystals of the blue bronze were obtained by electrolytic reduction of a $MoO_3 : K_2MoO_4$ melt in the mole ratio 3.35:1. MoO_3 was prepared by slowly heating $(NH_4)_2Mo_2O_7$ (Climax Molybdenum Co., total impurity content < 0.01 wt%) to $600^\circ C$ in a gold dish. K_2MoO_4 was prepared from the MoO_3 by precipitation from KOH solution (Fischer reagent grade KOH) and dried in an oven. Powder x-ray-diffraction patterns of both materials agreed with the American Society for Testing Materials (ASTM) files for MoO_3 and K_2MoO_4 . Mixtures of the MoO_3 and K_2MoO_4 in the above mole ratio were melted in air in a gold crucible and then reground at room temperature before electrolysis.

The electrolysis was carried out in a nested set of high-purity Coors alumina crucibles. The 20-ml inner crucible which had several small slits cut into it with a diamond saw to allow ion migration was fitted with an alumina cover through which was passed a four-hole alumina thermocouple-protection tube containing a Pt-10 at.%-Rh-Pt thermocouple and a Pt cathode. A Pt anode was placed in the 100-ml outer crucible. The nested crucible-electrode assembly containing the $MoO_3 : K_2MoO_4$ mixture was placed in a vertical-tube furnace of large thermal mass. Temperature was controlled by a voltage-regulated Variac and could be held anywhere between 550 and $560^\circ C$ to within $2^\circ C$ over a period of several days. Current for the electrolysis was provided by a 10-mA Weston constant-current supply.

At the end of the electrolysis period, the crucibles were quickly dumped of their molten contents leaving the bronze behind. In ten trials, three of which were successful in yielding the blue bronze, the bronze was found at the bottom of the inner crucible, not on the electrode. In some runs, argon gas was passed over the crucible assembly, but this did not appear to have an effect on obtaining the material. None of the runs yielded any red bronze even for a mole ratio of $MoO_3 : K_2MoO_4$ of 3.15:1 as used by Bouchard, Perlstein, and Sienko.¹⁰ In one run, in fact, the blue bronze appeared in the outer anode compartment as well as in the cathode compartment.

B. Electrical Measurements

Crystals for electrical measurements were picked out of the cathode compartments and oriented along the long b axis in a crystal holder to be described

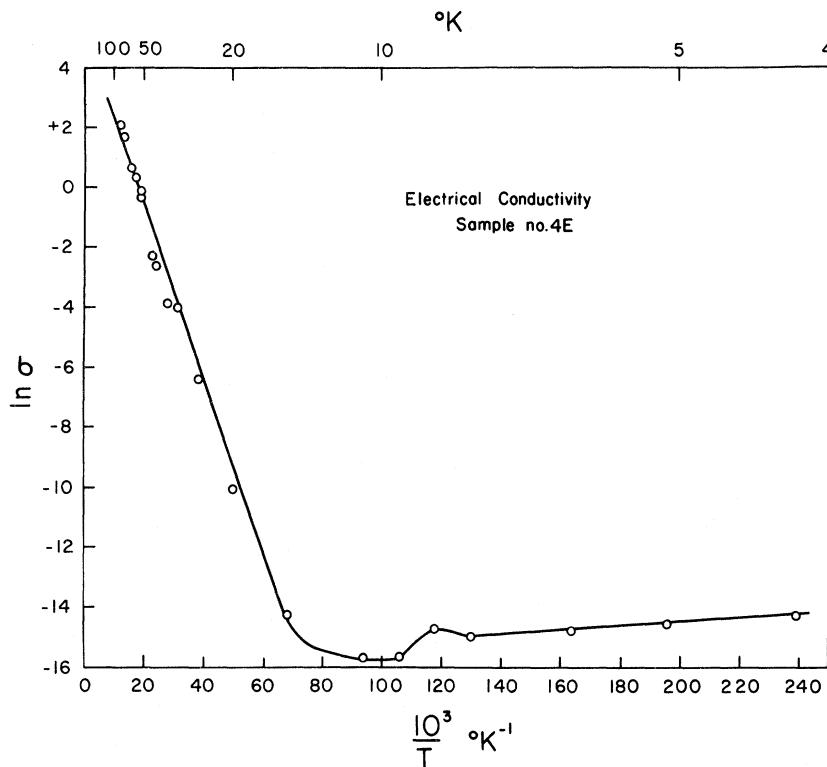


FIG. 4. Natural logarithm of the conductivity vs inverse temperature for $K_{0.30}MoO_3$; 4–81 °K (σ expressed in $\Omega^{-1} \text{ cm}^{-1}$).

elsewhere. Current contacts were made by soldering with indium. Potential contacts to the crystal were also made with indium. The crystal holder was placed in a liquid-helium cryostat in which the temperature could be cycled in a continuous manner between 4 and 300 °K. Temperature was measured with a Pt resistance thermometer and an Allen-Bradley $10\text{-}\Omega \frac{1}{2}\text{-W}$ carbon resistor, both mounted next to the sample.

Current leads for the crystal were placed in series with a set of standard resistors variable from 1 to $10^{11} \Omega$ and either a 1.35-V mercury battery or a 12-V lantern battery. Potential across the crystal was measured with a Leeds and Northrup K-5 potentiometer or a Keithley model No. 200b electrometer. Both forward and reverse current was employed to average out any thermal emfs. Below about 20 °K all samples showed a decidedly non-Ohmic response above a critical field. The low-temperature conductivity reported are for voltages below the critical value.

C. Results

The natural logarithm of σ vs $1/T$ for one representative sample is shown in Fig. 4 for T ranging from 4 to 81 °K. Figure 1 shows the results for one representative sample from 77 to 300 °K. The data of Fig. 1 is similar to that found by Bouchard *et al.*¹⁰ and Perloff, Vlasse and Wold.¹² The conductivity above 90 °K has an upward curvature with

a discontinuity in slope at 180 °K. There is no discontinuity in the conductivity itself. Below 90 °K the conductivity has a constant slope and then becomes weakly metallic below 10 °K. The conductivity at 4.2 °K is $6 \times 10^{-7} \Omega^{-1} \text{ cm}^{-1}$ and $7 \times 10^{+3} \Omega^{-1} \text{ cm}^{-1}$ at room temperature, representing a change of about ten orders of magnitude.

III. DISCUSSION

As indicated in Sec. I the ideal monoclinic crystal structure contains one $K_3 Mo_{10} O_{30}$ unit per lattice point. In the one-electron-band scheme, this would yield a metallic conductivity at all temperatures with strongly metallic behavior at very low temperatures contrary to the above observations.

Hall-effect measurements by Bouchard *et al.* show a change from n - to p -type conductivity around the 180 °K transition region. Their calculated data are shown in Table I. They offer the explanation that the blue bronze contains a normally filled valence band consisting of bonding $Mo-d(t_{2g})-O-p_r$ orbitals and an empty conduction band consisting of overlapping $Mo-d(t_{2g})$ orbitals only. Electrons from potassium would presumably occupy impurity donor levels below the conduction band. The changeover from n - to p -type conductivity is then explained as being due to formation of high-mobility holes in the valence band resulting from excitation of holes from impurity acceptors above 180 °K. Because the $d(t_{2g})-O-p_r$ valence band is expected to be wider

TABLE I. Hall data for $K_{0.30}MoO_3$.

Temperature (°K)	Hall Coefficient $R(\text{cm}^3/\text{C})$	Carrier density n or $p=1/Re$	σ ($\Omega^{-1} \text{cm}^{-1}$)	Hall mobility $\mu_H = R \sigma$ ($\text{cm}^2/\text{V sec}$)
74	-3.5	1.8×10^{18}	7.12	25
92	-7.7×10^{-1}	8.1×10^{18}	1.71×10^1	13
102	-2.9×10^{-1}	2.15×10^{19}	3.28×10^1	9.6
121	-5.3×10^{-2}	1.2×10^{20}	1.04×10^2	5.5
131	-2.5×10^{-2}	2.5×10^{20}	1.73×10^2	4.4
135	-1.6×10^{-2}	4.0×10^{20}	2.06×10^2	3.2
146	-1.2×10^{-3}	5.0×10^{21}	2.88×10^2	0.36
164	$\sim +1.5 \times 10^{-3}$	$\sim 4 \times 10^{21}$	8.5×10^2	~ 1
292	$+1.5 \times 10^{-3}$	4.2×10^{21}	2.52×10^3	3.8

than the $d(t_{2g})$ conduction band, the higher mobility of the holes will dominate the high-temperature conductivity.

We do not believe that this model adequately explains the data. Aside from the fact that the number of donors and acceptors would have to be as large as the potassium ion content of 4.7×10^{21} ions/cm³ to give the Hall data shown in Table I, each of the impurity states should contribute to the magnetic susceptibility. The molar susceptibility from 1.5 to 300 °K has been measured by Bouchard *et al.*¹⁰ and from 77 to 300 °K by Morris and Wold.¹¹ The results of Morris and Wold are shown in Fig. 5. Both workers find qualitatively the same shape for χ vs T with χ becoming temperature independent below 100 °K. However, as can be seen in Fig. 5, the results of Morris and Wold show χ changing from diamagnetic to paramagnetic behavior with increasing temperature, whereas for the data of Bouchard *et al.* the results are shifted upwards so that the low-temperature data show temperature-independent paramagnetism.

The Curie susceptibility for $4.7 \times 10^{21}/\text{cm}^3$ unpaired impurity spins at room temperature is about 430×10^{-6} emu/mole of bronze. The blue bronze, however, has a susceptibility of only $+7.7 \times 10^{-6}$ emu/mole at room temperature which decreases to even lower values at lower temperatures. Thus, if there were any large number of impurities, they would have to be spin paired.

This idea was postulated by Perloff *et al.*¹² They claim that the electrons from potassium are spin paired forming Mo(IV) sites. The conductivity is then explained by excitation of electrons from the Mo(IV) sites into a conduction band made up of antibonding $d(t_{2g})-p_r$ orbitals. This model presents some of the same problems as that of Bouchard *et al.* It doesn't seem likely that Mo(IV) should exist in a predominantly Mo(VI) lattice. Electron-electron repulsion should keep the electrons far apart. Even if severe local distortions favored such a species, the distortions should easily be seen in the temperature dependence of the x-ray data but no such distortion has been observed.^{12,13}

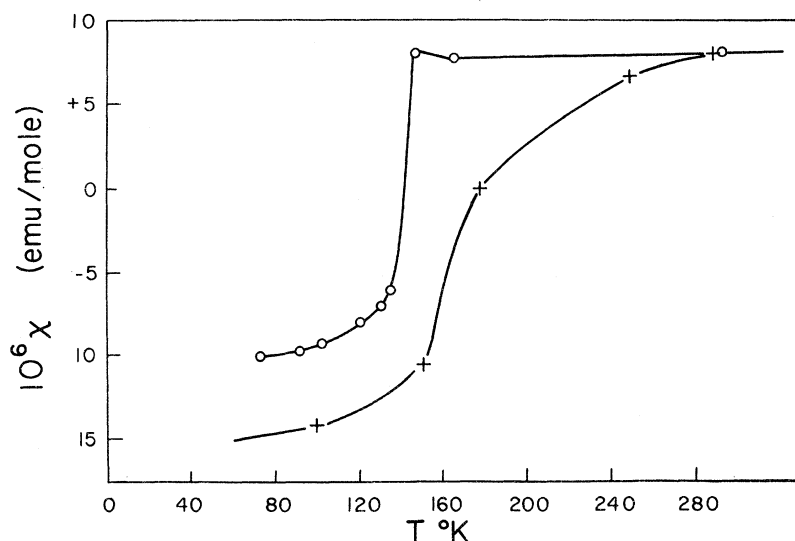


FIG. 5. Magnetic susceptibility vs temperature for $K_{0.30}MoO_3$. Experimental points (+) are those of Morris and Wold (Ref. 11). Theoretical curve (o) is for the excitonic-insulator model discussed in the text.

Aside from this, as the temperature is raised, uncoupling of the spins should occur as electrons are excited into the conduction band. Once again the full spin moment should be observed with increasing temperature. The susceptibility of Fig. 5 does not show this. Although it increases with increasing temperature, it always remains very small.

The change from semiconducting-to-metallic behavior at 180 °K is also not understandable in terms of the model of Perloff *et al.* unless one includes a screened short-range attractive interaction between the electron in the conduction band and the localized "hole" left behind in the donor state as described theoretically by Ramirez, Falicov, and Kimball.¹⁴ The peculiar behavior in the neighborhood of 180 °K could then arise from a continuous decrease in the effective gap between the localized levels and the conduction band with increasing temperature because of the temperature-dependent attractive interaction. This model appears to have a wide range of application depending on the strength of the electron-hole interaction but also depends on the presence of discrete localized states. There do not appear to be localized states in the blue bronze based on the magnetic-susceptibility results. Nevertheless, as pointed out by Doniach,¹⁵ the model of Ramirez *et al.* could also be applied to a set of localized antiferromagnetically coupled states. Although the details of this have not been worked out, one should still expect a heat effect associated with the total disordering of the antiferromagnetic state near 180 °K, but no such effect has been observed. Second, as each electron is excited from the antiferromagnetic state to a conduction band, the full spin moment of this electron should be observed in the susceptibility, which is not the case.

The same argument holds for a splitting of the expected half-filled band by a doubling of the periodicity due to antiferromagnetic coupling. The susceptibility should show a Néel point and there should be heat effects associated with the transition. No Néel point is observed and there are no obvious heat effects in differential-thermal-analysis experiments which could be attributed to a discontinuity in the specific heat.¹⁰

There are a number of other models which can be considered for the blue bronze, several of which we would like to discuss.

A. Mott-Hubbard Transition

Mott¹⁶ suggested that for a system with an odd number of electrons per lattice site, the ground state could be insulating if the Coulomb repulsion between electrons on neighboring sites was larger than the bandwidth formed by electron delocalization. Hubbard has formalized Mott's idea in a series of papers by employing a Hamiltonian which includes Coulomb repulsion between electrons on nearest-

neighbor sites.¹⁷ If this electron correlation energy is U , then the normally metallic half-filled band is split producing a full band separated by an empty band with an energy gap equal to U . A number of conditions would have to be met in order to apply this model to the blue bronze: (a) The Mott-Hubbard ground state must be antiferromagnetic to account for the low magnetic susceptibility of Fig. 5; and (b) there needs to be a short-range attractive interaction between electrons excited across the correlation energy gap and the empty "hole" states left behind as suggested by the model of Ramirez *et al.* in order to account for the shape of the conductivity curve at the transition point. Excitation of an electron from the Mott-Hubbard antiferromagnetic ground state across the correlation energy gap is equivalent to taking an electron from a lattice site with spin up, say, and placing it on a neighboring lattice site which has an electron with spin down. The effect of this on the magnetic susceptibility will thus be small since the conduction electron is: always coupled with an electron of opposite spin and the *two* hole states left behind on the vacant site are also spin paired. Although the details of the temperature dependence of the transport properties of this model have not been worked out, we can give a preliminary prediction for the lower limit of the semiconductor-to-metal transition temperature based on the model of Ramirez *et al.* These workers have shown that the semiconductor-to-metal transition temperature T_c , in which there is a short-range attractive interaction between a conduction electron and a localized hole state in a cubic lattice, is

$$kT_c = 0.177\Delta + 0.052W ,$$

where Δ is the band gap and W is the bandwidth. For the blue bronze the slope of the conductivity curve between 15 and 90 °K is 0.025 eV (Figs. 1 and 4) so that for a two-band model the band gap Δ will be twice this value or 0.050 eV. A lower limit for the bandwidth can be found by calculating a value of the electron relaxation time τ using a value of 25 cm²/V sec for the mobility at 74 °K from Table I, assuming an effective mass of one free-electron mass (which we will justify later) and requiring that W be greater than \hbar/τ . This gives a lower limit to the conduction bandwidth of 0.05 eV and thus a lower limit for the transition temperature of 133 °K.

It would thus appear that a Mott-Hubbard transition in which the ground state is antiferromagnetic and in which short-range electron-hole attraction is postulated can account for the semiconductor-to-metal transition in a qualitative way. There is, however, one feature of this model which seems unrealistic for the blue bronze. The lower limit of 0.05 eV placed on the bandwidth seems too small for a material with an effective mass of one free-electron

tron mass. A more realistic lower limit would be to calculate the minimum bandwidth from the relaxation time in the metallic region ($T > 180^\circ\text{K}$) using the room-temperature mobility from Table I. This gives $W > 0.3$ eV so that $W/U \gg 1$ and no Mott-Hubbard band splitting should be observed unless the bandwidth below the transition temperature is considerably reduced.

B. Excitonic-Insulator Model

Mott¹⁶ has also proposed that in a normal wide-band semiconductor, if the band gap is small enough, excitation of an electron from the valence band to the conduction band will produce electron-hole pairs which are correlated by the long-range Coulomb attraction. These excitons do not contribute to the conductivity. Even if the band gap is decreased to zero and becomes negative, the ground state remains insulating until the Coulomb attraction becomes a screened interaction at which point there is a transition to the semimetallic state.

This model has recently been formalized and the transport properties have been worked out for some limiting cases.¹⁸ The interesting feature of this model is the distinct possibility that a material which would be semimetallic at 0°K in terms of the one-electron-band approximation can, in fact, be an insulator or very weakly metallic if the excitonic state can be formed.

Since the semimetallic state is produced by partial overlap of a filled band with an empty band, thus producing an equal number of holes and electrons on either side of the Fermi level, it is necessary to have an even number of electrons per lattice point. The blue bronze does not fit this picture if the stoichiometry is $\text{K}_{0.30}\text{MoO}_3$ (or $\text{K}_3\text{Mo}_{10}\text{O}_{30}$). It is possible, however, that the stoichiometry is such that not all oxygen sites are filled. For instance, if the stoichiometry were $\text{K}_{0.30}\text{MoO}_{2.95}$ (or $\text{K}_3\text{Mo}_{10}\text{O}_{29.5}$) corresponding to one oxygen missing for every two $\text{Mo}_{10}\text{O}_{30}$ clusters, then each cluster would have an even number of electrons. It could be argued that, for any one sample, such a stoichiometry would be coincidental and that the potassium and/or oxygen content could vary from sample to sample over a wide range. We point out, however, that the blue bronze can be synthesized only over an extremely narrow region of the MoO_3 - K_2MoO_4 phase diagram as shown by Wold *et al.*⁷ and within that region the temperature at which the bronze appears may vary by only 10 - 20°C . It is thus possible that there is a very sharp minimum in the free energy at that composition which gives four electrons/cluster.

The original analysis of Wold's group indicated a stoichiometry $\text{K}_{0.27}\text{MoO}_{2.94}$ which corresponds to 3.95 electrons per cluster. Analysis by Bouchard *et al.*¹⁰ did not confirm this but within their error

four electrons per cluster is still possible. We therefore wish to suggest a model in which there is an indirect negative band gap between the Brillouin zones leading to a semimetallic condition. In the blue bronze the overlap is sufficient to allow the formation of about 4×10^{21} electrons and holes per cubic centimeter on either side of the Fermi level above the 180°K transition temperature. At 0°K , the majority of this large number of electrons and holes are bound in excitons. As the temperature is raised, the excitons are thermally broken to form conducting electrons and holes on either side of the Fermi surface. As more uncorrelated electrons and holes are produced with increasing temperature, the exciton binding energy decreases because of the screened potential until at a critical temperature, the excitonic state vanishes and the conductivity is then dominated only by changes in the mobility of the electrons and holes.

One of the features of this model is that the maximum possible transition temperature will be of the same order of magnitude as the 0°K exciton binding energy E_b . E_b is determined by treating the exciton as a simple hydrogenlike atom with inclusion of the static dielectric constant of the medium and the fact that the effective mass is the reduced effective mass of the electron-hole pair. Thus,

$$E_b = (\mu^*/m)(1/\epsilon_0^2)(e^2/2a_0) \quad (1)$$

Here μ^* is the reduced effective mass, m the free-electron mass, ϵ_0 the static dielectric constant, and $e^2/2a_0 = 13.61$ eV, the ionization potential for the hydrogen atom. We will assume that the electron and hole effective masses in the blue bronze are identical (which is probably not true because of the anisotropic nature of the bronze) and estimate their value from the Pauli-Peierls equation for the magnetic susceptibility χ of a degenerate system with a spherical Fermi surface (also not true for a semimetal),

$$\chi = \frac{4Mm^*\mu_0^2}{h^2d} (3\pi^2n)^{1/3} \left(1 - \frac{m_0^2}{3m^{*2}}\right) \frac{\text{emu}}{\text{mole}},$$

where μ_0 is the Bohr magneton, n the electron or hole density, m_0/m^* the ratio of free-electron mass to effective mass, and M/d the ratio of molecular weight (156) to density (4.26 g/cm³). Using Morris and Wold's room-temperature value of $\chi = 7.7 \times 10^{-6}$ emu/mole and taking $n = 4.2 \times 10^{21}$ /cm³ from Table I, we find $m^* = 0.95m_0$. The static dielectric constant¹⁹ of MoO_3 is 18.0 so that the exciton binding energy from Eq. (1) is

$$E_b = 0.021 \text{ eV}, \quad (2)$$

which is equivalent to a temperature of 244°K . The observed transition temperature of 180°K is thus less than the excitonic binding energy as should be

expected if the excitonic-insulator model is to be applicable.

It should be pointed out here once more that the excitonic insulator on the semimetallic side shows the unusual feature that the electrons and holes which are thermally generated with increasing temperature are always degenerate, but the number of such degenerate particles increases with increasing temperature (a discussion of this point has been given by Kohn).^{18(a)} In Secs. III C-III G we will apply this unusual feature of the excitonic insulator in a semiquantitative way to the various experimental parameters that have been determined for the blue molybdenum bronze.

C. Magnetic Susceptibility

The excitonic-insulator model predicts the general behavior of the magnetic susceptibility for the blue bronze. At low temperatures, the majority of electrons and holes are bound in singlet exciton formation so that the susceptibility should be just the diamagnetism of the electron-hole pair.

We estimate the diamagnetism of the exciton from the calculated value of -2.37×10^{-6} emu/mole for the diamagnetism of the hydrogen atom.²⁰ This value must be corrected by inclusion of the dielectric constant of the medium and the reduced mass of the exciton giving

$$\begin{aligned}\chi_{\text{exciton}} &= -(2.37)(2)(18)^2 \times 10^{-6} \\ &= 1536 \times 10^{-6} \text{ emu/mole.}\end{aligned}$$

Taking the number of excitons to be equal to the room-temperature number of holes of $4.2 \times 10^{21}/\text{cm}^3$ from Table I, the susceptibility of the excitons is

$$\begin{aligned}\chi_{\text{excitons}} &= -\frac{1536 \times 10^{-6}}{6.02 \times 10^{23}} (4.2 \times 10^{21}) \\ &= -10.7 \times 10^{-6} \text{ emu/mole.}\end{aligned}$$

This value is to be compared with the extrapolated value from Morris and Wold's data of -15×10^{-6} emu/mole shown in Fig. 5. (The background corrections for the ionic cores is almost zero since 0.3K^+ contributes²⁰ -3.9×10^{-6} emu/mole and an MoO_3 network contributes $+3 \times 10^{-6}$ emu/mole.²¹ The total correction is thus negligible and has been neglected here as well as by Morris and Wold.²²)

The temperature dependence of the magnetic susceptibility for the blue bronze will then consist of two parts; the Pauli-Peierls contribution (a sum of the degenerate paramagnetism and the diamagnetism of the free electrons and holes) which increases with temperature as $n^{1/3}$ and, second, the diamagnetism of the excitons which decreases with increasing T (since the number of excitons is decreasing). Figure 5 shows a comparison between the experimental magnetic susceptibility and the

predicted susceptibility. The values of n used to calculate the predicted susceptibility were taken from Table I. Although the agreement is poor as would be expected since the Fermi surface near the zone edge is not spherical, the magnitudes and the general temperature dependence is correct.

D. Seebeck Coefficient

For a metal with a spherical Fermi surface the Seebeck coefficient is²³

$$S = -\frac{(6.2 \times 10^{-2})(8m^*)}{h^2} \left(\frac{\pi}{3n}\right)^{2/3} \frac{T\mu V}{^\circ\text{K}} \quad (3)$$

For the excitonic insulator at low temperatures, the number of degenerate carriers is small and thus S is predicted to be large. n increases with increasing T as the excitons are thermally ionized producing additional degenerate electrons and holes. At the transition temperature n is very large and thus S should be very small.

Figure 6 shows a plot of S vs T for Eq. (3). The values of n were taken from Table I with the assumption that electrons make the major contribution to S . The experimental Seebeck coefficient data of Bouchard *et al.*¹⁰ is also shown for comparison. Over the limited range of the experimental data the comparison is satisfactory.

E. Electrical Conductivity

The electrical transport properties of the excitonic insulator have been worked out in the case of zero scattering by Jérôme, Rice, and Kohn²⁴ and for impurity scattering by Zittartz.²⁵ Both these calculations predict an upward curvature for σ with increasing temperature with a discontinuity in the slope at the transition temperature. The blue bronze follows exactly this behavior as seen in Fig. 1. Jérôme *et al.* predict an infinite slope on the low-temperature side of the transition, whereas Zittartz shows that the inclusion of impurity scattering produces a finite slope at the transition. The impurity-scattering potential has opposite effects on an electron and hole so that the presence of impurities reduces the effective electron-hole attraction. The effects of phonon interactions with the excitons, in particular optical-mode phonons, which should be the dominant scattering mechanism in this polar material, does not appear to have been studied at this time. The slope of the conductivity curve is nevertheless finite on the low-temperature side of the transitions as can be seen in Fig. 1. That the slope of the conductivity curve is governed by the change in carrier density and not some peculiarity in the mobility is shown in Fig. 7 where $\ln \sigma$ vs $1/T$ is plotted using the data from Table I. The general shape of Figs. 1 and 7 are the same. The conductivity changes by eight orders of magnitude between 77 and 180 °K and so does the carrier

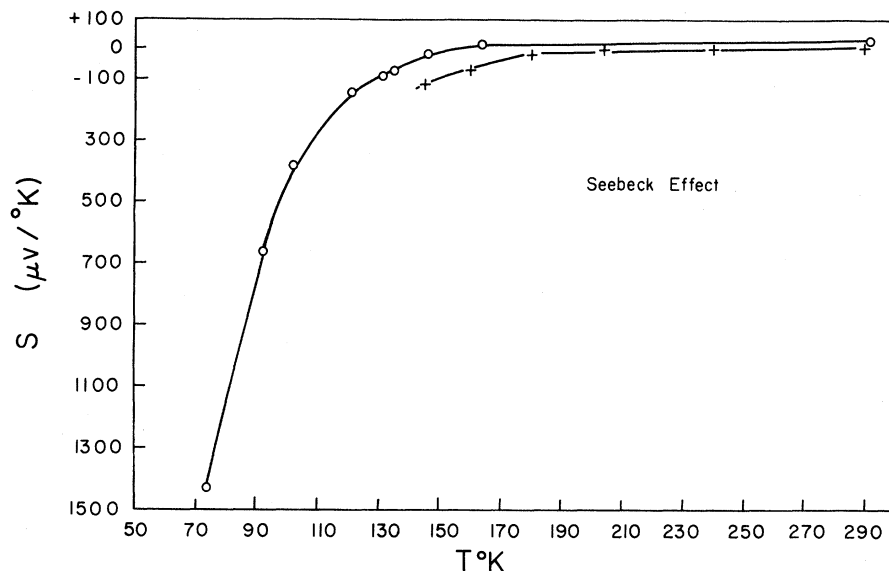


FIG. 6. Seebeck coefficient vs temperature for $K_{0.30}MoO_3$. Experimental points (+) are those of Bouchard, Perlstein, and Sienko (Ref. 10). Theoretical curve (o) is for the excitonic-insulator model.

density.

Zittartz shows that there is a critical value of the relaxation time τ due to impurity scattering such that if $h\tau^{-1}/E_b > 1$ the excitonic phase is not formed. This condition implies that the frequency of impurity-scattering events should be small compared to the frequency of exciton formation, otherwise the excitonic state will not have a chance to form. For the blue bronze, the impurity content is $< 0.01\%$ as indicated in Sec. II. This corresponds to an impurity density N of about 10^{18} atoms/cm³.

Using Erginsoy's analysis for neutral impurity scattering²⁶

$$\tau = m^*{}^2 e^2 / 20\hbar^3 \epsilon_0 N,$$

we estimate the ratio $h\tau^{-1}/E_b$ to be 0.4 so that even in the presence of this large impurity content the excitonic phase is stable.

Zittartz has also shown that for temperatures well below the transition temperature,

$$\sigma \propto e^{-E_b/kT} / E_b T,$$

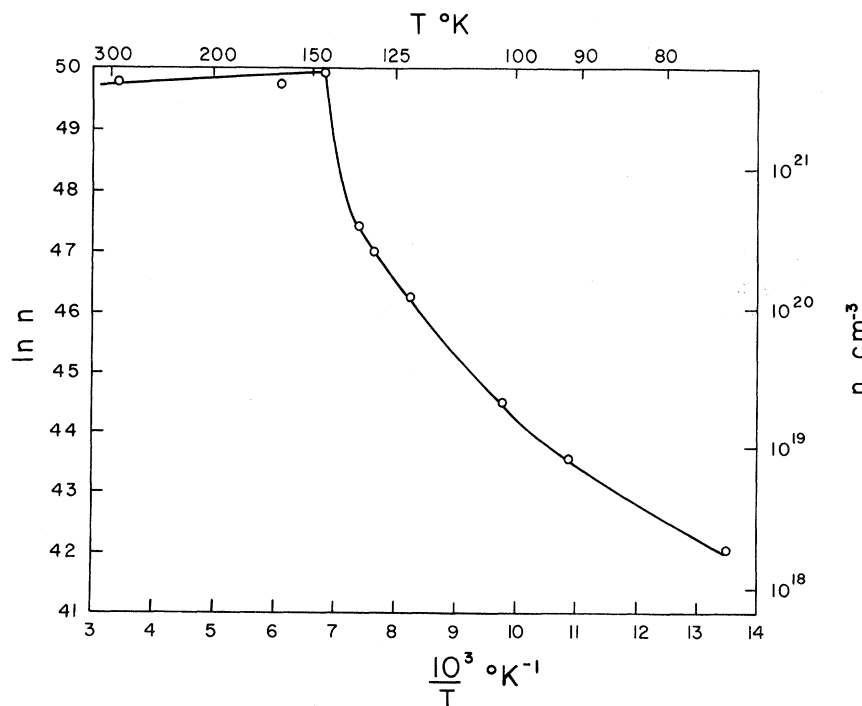


FIG. 7. Natural logarithm of the carrier density vs inverse temperature for $K_{0.30}MoO_3$. Data taken from Table I.

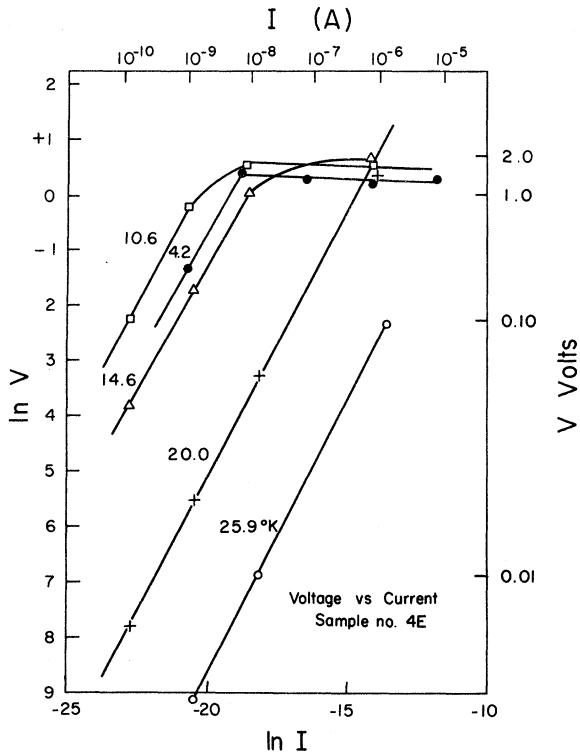


FIG. 8. Natural logarithm of voltage vs natural logarithm of current for sample of Fig. 4. Non-Ohmic behavior is apparent below 20 °K.

so that if $kt < E_b$, a plot of $\ln \sigma$ vs $1/T$ will be a straight line with slope E_b . Figure 4 shows this to be the case for the blue bronze in the temperature range 15 to 90 °K. The slope of the conductivity plot in this region is, in fact 0.025 eV which is to be compared with the estimate of the exciton binding energy of 0.021 eV derived from Eq. (1).

F. Low-Temperature Non-Ohmic Behavior

Figure 8 shows the dependence of the voltage on current for low temperatures. It can be seen that as the temperature is lowered, there is a critical voltage above which non-Ohmic behavior sets in. The current at which the non-Ohmic behavior occurs shifts to lower values the lower the temperature. The shape and temperature dependence of these curves, as well as the low critical voltage at which the non-Ohmic behavior appears, are similar to the curves for impact ionization of neutral impurities that occurs in elemental semiconductors like germanium.²⁷ Since the bound electron-hole pair in the blue bronze is essentially a neutral impurity with a radius

$$r = \hbar^2 \epsilon_0 / \mu^* e^2 \approx 18 \text{ \AA} , \quad (4)$$

it is tempting to speculate that the non-Ohmic behavior that is observed is due to impact ionization of the excitons. Such a process would require that the excitons interact strongly enough with the lattice so that electron exciton scattering be reasonably elastic to allow the free electrons (or holes) to gain sufficient energy from the electric field for the ionization process to occur. As long as the exciton density remains high, the non-Ohmic behavior should manifest itself to even higher temperatures than shown in Fig. 8 (possibly to 100 °K).

G. Summary and Conclusions

The semiconductor-to-metal transition which occurs at 180 °K in the blue molybdenum bronze has been interpreted in terms of an electron-hole correlation model which produces an insulating ground state at low temperatures. The interesting feature of this model is the fact that the ground state consists of bound electron and holes producing singlet excitons which carry no current. With increasing temperature, ionization of the excitons produces degenerate electrons and holes on either side of the Fermi surface. With increasing temperature, the exciton binding energy diminishes due to more effective screening of the bound electrons and holes by the free charge carriers. Eventually, the exciton binding energy goes to zero giving the appearance of a semiconductor-to-metal transition which occurs at 180 °K for the blue molybdenum bronze. The fact that the free charge carriers are degenerate at all temperatures offers an explanation for the weak temperature dependence of the magnetic susceptibility and for the Seebeck coefficient. Unfortunately, since the formation of the excitonic state can be accompanied by a lattice distortion in the presence of strong electron-phonon coupling,^{18(c)} it is not obvious that this model is easily distinguishable from one in which two overlapping bands simply uncross due to a lattice distortion *without* an electron-hole interaction. In fact, for $K_3\text{Mo}_{10}\text{O}_{30}$ with three electrons per lattice point, a new Brillouin zone could form at the Fermi surface by a doubling of the periodicity due to a small distortion of the $\text{Mo}_{10}\text{O}_{30}$ clusters. The semiconductor-to-metal transition could then be realized without invoking electron-hole correlation. Attempts to find a lattice distortion by x-ray analysis, however, have not been successful.^{12,13} We therefore suggest the excitonic-insulator model only as a tentative explanation for the properties of the blue molybdenum bronze. It would be of interest to see if the infrared optical properties of the blue bronze are metalliclike below the semiconductor-metal transition temperature as suggested here or whether an absorption edge occurs. It is known that a strong photoconductive response is observed¹⁰ at 77 °K but the wavelength dependence has not been studied.

ACKNOWLEDGMENT

We wish to acknowledge the many helpful discus-

sions with Dr. Aaron Bloch of this department on the theoretical aspects of this problem.

¹For a review of the bronzes, see M. J. Sienko, in *Non-Stoichiometric Compounds*, edited by Robert F. Gould (American Chemical Society, Washington, D. C., 1963) Advances in Chemistry Series No. 39, p. 224; H. R. Shanks, P. H. Sidles, and G. C. Danielson, *ibid.*, p. 237; P. G. Dickens and M. S. Whittingham, *Quart. Rev.* **22**, 30 (1968).

²J. B. Goodenough, *Czech. J. Phys.* **B17**, 304 (1967).

³B. L. Crowder and M. J. Sienko, *J. Chem. Phys.* **38**, 1576 (1963).

⁴J. H. Perlstein and M. J. Sienko, *J. Chem. Phys.* **48**, 174 (1968).

⁵J. B. Goodenough, *J. Solid State Chem.* **1**, 349 (1970).

⁶T. A. Bither, J. L. Gillson, and H. S. Young, *Inorg. Chem.* **5**, 1559 (1966).

⁷A. Wold, W. Kunmann, R. J. Arnott, and A. Ferretti, *Inorg. Chem.* **3**, 545 (1964).

⁸J. Graham and A. D. Wadsley, *Acta Cryst.* **20**, 93 (1966).

⁹N. C. Stephenson and A. D. Wadsley, *Acta Cryst.* **19**, 241 (1965).

¹⁰G. H. Bouchard, Jr., J. Perlstein, and M. J. Sienko, *Inorg. Chem.* **6**, 1682 (1967).

¹¹B. L. Morris and A. Wold, *Rev. Sci. Instr.* **39**, 1937 (1968).

¹²D. S. Perloff, M. Vlasse, and A. Wold, *J. Phys. Chem. Solids* **30**, 1071 (1969).

¹³D. S. Perloff, Ph.D. thesis (Brown University, 1969), p. 52 (unpublished).

¹⁴R. Ramirez, L. M. Falicov, and J. C. Kimball, *Phys. Rev. B* **2**, 3383 (1970); L. M. Falicov and J. C. Kimball, *Phys. Rev. Letters* **22**, 997 (1969).

¹⁵S. Doniach, *Advan. Phys.* **18**, 819 (1969).

¹⁶N. F. Mott, *Phil. Mag.* **6**, 287 (1961).

¹⁷For a review and references to the Mott-Hubbard model, see D. Adler, *Solid State Phys.* **21**, 1 (1968).

¹⁸For a review of the properties of the excitonic insulator, see (a) W. Kohn, *Phys. Rev. Letters* **19**, 439 (1967); (b) B. I. Halperin and T. M. Rice, *Rev. Mod. Phys.* **40**, 755 (1968); (c) *Solid State Phys.* **21**, 116 (1968).

¹⁹S. K. Deb and J. A. Chopoorian, *J. Appl. Phys.* **37**, 4818 (1966).

²⁰P. W. Selwood, *Magnetochemistry* (Interscience, New York, 1956), p. 71.

²¹J. Baudet, *J. Chim. Phys.* **58**, 853 (1961).

²²A. Wold (private communication).

²³H. Jones, in *Encyclopedia of Physics*, edited by M. Flügge (Springer, Berlin, 1956), Vol. 19, p. 276.

²⁴D. Jérôme, T. M. Rice, and W. Kohn, *Phys. Rev.* **158**, 462 (1967).

²⁵J. Zittartz, *Phys. Rev.* **165**, 605 (1968).

²⁶C. Erginsoy, *Phys. Rev.* **79**, 1013 (1950).

²⁷N. Sclav and E. Burstein, *J. Phys. Chem. Solids* **2**, 1 (1957).

Wavelength-Modulation Spectra and Band Structures of InP and GaP

Carmen Varea de Alvarez, *† John P. Walter, *‡ Marvin L. Cohen, * J. Stokes, and Y. R. Shen

Department of Physics, University of California, Berkeley, California 94720
and Inorganic Materials Research Division, Lawrence Berkeley Laboratory,
Berkeley, California 94720
 (Received 24 January 1972)

Modulated-reflectivity measurements of InP and GaP at 5, 77, and 300 °K are compared with empirical-pseudopotential calculations of the electronic band structure, the imaginary part of the frequency-dependent dielectric function, and the derivative of the reflectivity.

I. INTRODUCTION

Modulated-reflectivity measurements have become one of the most accurate methods for the determination of critical points in the band structure of diamond- and zinc-blende-type semiconductors. Semiempirical calculations using the data these experiments provide have been highly successful in describing the electronic structure of these materials.^{1,2} In this paper we combine these techniques to study InP and GaP.

The modulated-reflectivity measurements for cubic InP and GaP crystals were done at 5, 77, and 300 °K. The results appear in Figs. 1 and 2

and the experimental procedure is described in Sec. II. Using the experimental data at 5 °K we have obtained the band structure of InP using the empirical-pseudopotential method (EPM).¹ We have also calculated the imaginary part of the frequency-dependent dielectric function $\epsilon_2(\omega)$, the reflectivity $R(\omega)$ and the modulated-reflectivity spectra $R'(\omega)/R(\omega)$ which are compared directly with experiment. Spin-orbit corrections in InP are small and are not included; their effects are discussed by comparison with other zinc-blende crystals.³

We have made an analysis of the critical points of the calculated optical structure to identify the